Merits and Limitations of Automotive Radar for Land Vehicle Positioning in Challenging Environments

Emma Dawson, Eslam Mounier, Mohamed Elhabiby, and Aboelmagd Noureldin, *Senior Member, IEEE*

***Abstract*—Land vehicles of the near future require accurate positioning systems that are robust across diverse and changing environmental conditions. While global navigation satellite systems (GNSSs) remain standard for absolute positioning on land, access to satellite signals is unreliable or absent in many urban environments. Inertial navigation systems (INSs) can provide positioning solutions capable of bridging short GNSS outages but cannot sustain adequate positioning accuracy for the duration of outages often present in cities. The need for vehicles to navigate reliably through such environments has motivated research into multisensor fusion for positioning. Aiding sensors include cameras, light detection and ranging (LiDAR), and radar. Due to the varying effects of environmental conditions on each type of sensor, more than one sensor system must be implemented. Radars are an attractive automotive sensor due to their insensitivity to adverse lighting conditions, which affects cameras, and inclement weather, which impacts both cameras and LiDAR. Automotive radars are low-cost sensors found in most modern vehicles, applied widely for driver assistance systems. Recent advancements in radar technology, however, have led to research in radar-based positioning. This article presents a comparative case study and analysis of two radar-based positioning methods across three practical driving scenarios. Radar odometry and radar-to-map registration are applied to real driving scenarios, including a university campus, a busy shopping street, and an indoor parking garage. Areas where radar-based positioning fails are discussed, aiming to identify challenges faced specifically by automotive radar. In addition, areas where radar-based navigation is already performing robustly are presented.**

***Index Terms*— Automotive radars, electronic scanning radar (ESR), global navigation satellite system (GNSS), inertial navigation system (INS), iterative closest point (ICP), map registration, positioning.**

I. Introduction

ADVANCEMENTS in technology for autonomous vehicles (AVs) have brought attention to the need for high-precision positioning (50 cm at 95%) across all weather and environmental conditions [1]. Global navigation satellite systems (GNSSs) can provide precise positioning services when access to satellite signals is available. However, in urban environments, satellite signals are often limited, degraded, or entirely unavailable [2]. To bridge instances of GNSS signal outages, AVs are equipped with inertial navigation systems (INSs), dead-reckoning navigation systems advantageous due to their self-contained nature [3], [4]. INS is capable of maintaining good short-term positioning accuracy when GNSS is unavailable but suffers from position drift in the longer term. Multiple sensor systems must therefore be relied upon to satisfy the positioning requirements of AVs.

Additional sensor systems commonly considered for AV navigation include cameras, light detection and ranging (LiDAR), and radar. However, vision-based navigation does not perform well when the camera images are degraded by poor lighting and bad weather [5]. While LiDARs perform well independently of lighting conditions, they suffer in rain and fog as the light emitted by the LiDAR is refracted as it passes through the water particles [5].

Radars are low-cost sensors found in most modern vehicles and used in advanced driver-assistance systems (ADASs) [6].

Manuscript received 3 August 2023; revised 18 September 2023; accepted 18 September 2023. Date of publication 27 September 2023; date of current version 31 October 2023. This research is supported by grants from the Natural Sciences and Engineering Research Council of Canada (NSERC) under grant numbers: RGPIN-2020-03900 and ALLRP-560898-20. The associate editor coordinating the review of this article and approving it for publication was Dr. Tai Fei. *(Corresponding author: Emma Dawson.)*

Emma Dawson and Eslam Mounier are with the Department of Electrical and Computer Engineering, Faculty of Engineering and Applied Science, Queen's University, Kingston, ON K7L 3N6, Canada (e-mail: emma.dawson@queensu.ca).

Mohamed Elhabiby is with Micro Engineering Tech, Inc., Calgary, AB T2M 0L7, Canada.

Aboelmagd Noureldin is with the Department of Electrical and Computer Engineering, Royal Military College of Canada (RMCC), Kingston, ON K7K 7B4, Canada.

Digital Object Identifier 10.1109/JSEN.2023.3318069

Automotive radars are unaffected by poor lighting and weather conditions, giving the radar an advantage over LiDAR and cameras in such scenarios. In addition, radar systems can measure instantaneous velocity information from all returned targets, which LiDAR cannot. Radar has a lower resolution than the aforementioned sensors, but when used in conjunction with INS, it is an emerging sensor capable of providing promising and high-accuracy navigation solutions [1].

A. Background

Radars, which can be fixed to a vehicle, are either automotive-type radars or scanning radars. More resolution is provided by the scanning radar, but it is also susceptible to higher levels of noise than the automotive radars [7]. The automotive radars can easily be integrated into the body of a vehicle, whereas the scanning radar must sit atop the vehicle, posing certain design limitations. Radars offer multiple possible strategies to solve positioning and navigation problems. The strategies can be generally divided into ego-motion estimation methods and mapping methods [8].

1) *Ego-Motion Estimation:* The problem of estimating the angular and forward velocity of a moving platform. These velocities can be integrated to provide an updated estimate of the platform's position in a navigation frame given a starting position or used in conjunction with map-based methods [6], [9], [10].
2) *Map-Based Methods:* Registration of radar scans with preexisting maps of the environment. This can provide a precise navigation update and relies on a dense radar point cloud as well as up-to-date, high-resolution maps [1], [11], [12].

B. Related Work

Recent work has explored radar-based navigation for both scanning and automotive radar.

Automotive radar localization using iterative closest point (ICP) to register radar scans to a preexisting map is presented in [13]. The map is created using radar detections in Universal Transverse Mercator (UTM) coordinates and georeferenced using real-time kinematic global positioning system (RTK-GPS). The algorithm is tested on a single trajectory consisting of a suburban and highway environment. A radar map is also created in [1] by aggregating detections of automotive radars from multiple passes of a vehicle through a trajectory. Localization is then performed using data from an additional pass through the trajectory, registering batches of radar scans to the radar map using a correlation-maximization-based algorithm. Through integration with inertial systems, an accuracy of 50 cm is achieved in an urban environment. ICP-based radar-to-street map localization methods are investigated in [11]. Information from OpenStreetMaps (OSMs) is used to build the map used for registration. To do so, corner points of buildings are considered and taken to formulate mathematical lines to be used as the feature model for the map matching problem. Cen and Newman [12], [14] proposed a robust data association algorithm based on key-point extraction and scan matching followed by rigid body transformations. However, they rely upon a scanning radar more sophisticated than what is expected to be available in an autonomous land vehicle.

Feature extraction from radar point clouds has been applied to simultaneous localization and mapping (SLAM). In [15], a 2-D occupancy grid map is constructed using automotive radar and shows real-time capability. Positioning accuracy of sub-1.2 m is achieved across two driving scenarios, consisting of a parking lot and a driveway. Relying on a scanning radar, feature matching and pose tracking are implemented in [16] using a probabilistic radar point cloud created from scanned radar images.

Instantaneous ego-motion estimation for radars has been investigated in [9], [10], and [17]. They have been shown to provide reliable forward velocity estimates, with difficulty providing angular velocity updates.

In general, real testing of radar-based navigation methods has been limited to repeated passes through the same trajectory or constrained to environments such as driveways, parking lots, and suburban environments, which present few dynamic challenges. An analysis of general radar-based navigation methods tested across diverse driving scenarios would allow a deeper understanding of the potential of automotive radars as an aiding sensor for AV navigation.

C. Objectives

The objective of this article is to look closely at the behavior of automotive radar-based navigation systems across multiple practical driving scenarios. The objectives are broken down as follows.

1) Investigate the performance of radar-based map matching in uncontrolled environments.
2) Identify challenging areas, conditions, or factors, areas where radars are likely to fail and areas where radars excel.

D. Contributions

The chief contributions of this article are summarized as follows.

1) Radar-based positioning demonstrated and assessed on multiple real, driving scenarios "in the wild."
2) Navigation using preexisting maps that were not constructed using the same setup used for navigation.

There is a lack of datasets that include automotive radar, which is also focused on research into vehicular positioning and navigation (there are several rich datasets specialized toward perception and object identification). The work in this article aims to fill that gap by providing insight into the behavior of radar-based algorithms in real-world driving scenarios.

II. Implementation Framework

Two automotive radar-based positioning strategies are examined in this work: radar odometry and radar scan-to-map registration. Radar odometry is dependent on the measured Doppler velocities and azimuths of targets, whereas map registration requires only the spatial positions of detected targets. Sections II-A and II-B provide an overview of the odometry and registration methods employed for this analysis.

A. Radar Odometry

Radar odometry requires the azimuth and Doppler velocity measurements from all radar targets in a scan. The odometry must be performed individually for each radar sensor because the velocity of the radar is dependent on the mounting location on the vehicle [17]. The Doppler and relative velocities of a detected target are given by

$$V_{D,i} = V_{\mathrm{Rx},i}\cos(\theta_i) + V_{\mathrm{Ry},i}\sin(\theta_i) \tag{1}$$

where $V_{D,i}$ and θ_i are the measured Doppler velocity and azimuth for a detected target i, respectively, and $V_{\mathrm{Rx},i}$ and $V_{\mathrm{Ry},i}$ are the relative velocities of the target with respect to the radar, in the x- and y-directions of the radar reference frame, respectively.

A radar scan of length N detections results in the following set of equations:

$$\begin{bmatrix} -V_{D,1} \\ \vdots \\ -V_{D,N} \end{bmatrix} = \begin{bmatrix} \cos\theta_1 & \sin\theta_1 \\ \vdots & \vdots \\ \cos\theta_N & \sin\theta_N \end{bmatrix} \begin{bmatrix} V_{\mathrm{Sx}} \\ V_{\mathrm{Sy}} \end{bmatrix} \tag{2}$$

where the radar sensor velocities V_{Sx} and V_{Sy} are equal and opposite to the corresponding relative velocities. The result is a system of equations consisting of as many equations as there are objects in the radar scan. Equation (2) is solved for V_{Sx} and V_{Sy} using a random sample consensus (RANSAC) algorithm [18]. V_{Sx} and V_{Sy} are then transformed to the forward velocity of the vehicle using the mounting location of the radar sensor [9].

B. Radar-to-Map Registration

An ICP [19] matching algorithm is implemented to register radar scans to a prebuilt map, providing position corrections to the vehicle. The following modules are required:

1) an INS mechanization;
2) an aggregated point cloud from the radar scans;
3) a point cloud representing the map of the environment.

An overview of the algorithm is presented in Fig. 1.

The components of Fig. 1 and the methods applied in this work to the above three modules are discussed in the following.

1) Inertial Mechanization: Inertial mechanization is necessary to pretransform the current radar scan from the vehicle frame into the navigation frame of the map. The INS mechanization model used in this article in a reduced inertial sensor system (RISS) [4]. The RISS model is implemented in the local 2-D Cartesian frame of the map. It outputs an updated position and azimuth (x_t, y_t, A) in the map frame at each timestep t.

2) Radar Point Cloud: A radar point cloud must be created as input to the ICP algorithm. Radar scans are received consisting of detections from all radars on the vehicle. A single four-radar scan is very sparse, even in a feature-rich environment [1]. Radar scans must therefore be aggregated to generate a point cloud, which can adequately represent the environment of the vehicle. The scans are aggregated in a sliding window of 1 s, resulting in a radar point cloud consisting of 20 scans when the radars are operating at 20 Hz. Each new scan is added

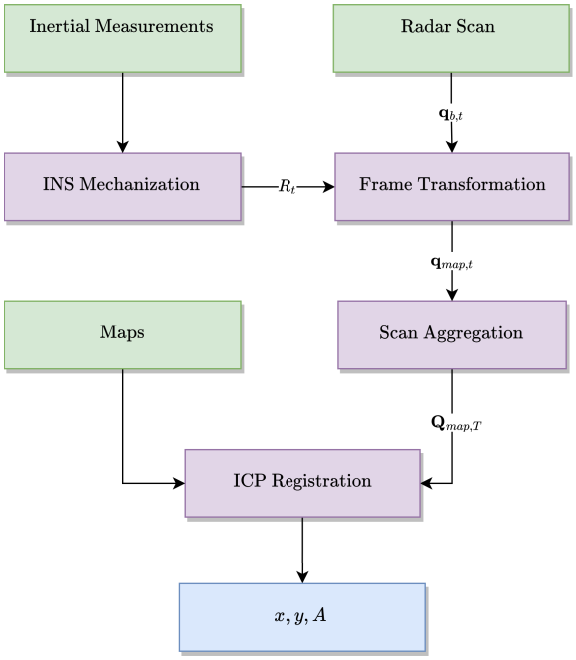

Fig. 1. Radar-to-map registration.

to the aggregated point cloud by transforming the scan into the map frame using the most recent INS update. At time t, the transformation matrix R_t is constructed using the current position and heading of the vehicle

$$R_t = \begin{bmatrix} \cos A_t & -\sin A_t & x_t \\ \sin A_t & \cos A_t & y_t \\ 0 & 0 & 1 \end{bmatrix} \tag{3}$$

where x and y correspond to the 2-D position of the vehicle within the map, respectively, and A is the azimuth. R_t transforms the radar point cloud from the vehicle frame, $\mathbf{q}_{b,t}$, into the map frame following the equation:

$$\begin{bmatrix} \mathbf{q}_{\mathrm{map},t} & \mathbf{0}_{M\times 1} & \mathbf{1}_{M\times 1} \end{bmatrix} = R_t \begin{bmatrix} \mathbf{q}_{b,t} & \mathbf{0}_{M\times 1} & \mathbf{1}_{M\times 1} \end{bmatrix}^{\top} \tag{4}$$

where M is the size of the point cloud. The radar scan is now in the map or navigation frame. This scan $\mathbf{q}_{\mathrm{map},t}$ is aggregated to the radar point cloud $\mathbf{Q}_{\mathrm{map},T}$ by appending it to the point cloud and dropping the oldest radar scan.

3) Map Point Cloud: A 2-D point cloud is used as a map. In the case of the outdoor environments, vertices from buildings are extracted from open data from the City of Kingston. Lines are interpolated between vertices of buildings at a resolution of 10 cm, generating a 2-D point cloud in UTM coordinates. Positioning takes place within the local coordinate system of this map.

III. Experimental Setup

All data presented in this article were collected by the Navigation and Instrumentation (NavINST) Laboratory at the Royal Military College of Canada, Kingston, ON, Canada, using a test vehicle fit with a suite of automotive sensors. Fig. 2 shows the test vehicle and a close-up of the test bed used to collect sensor data for the trajectory.

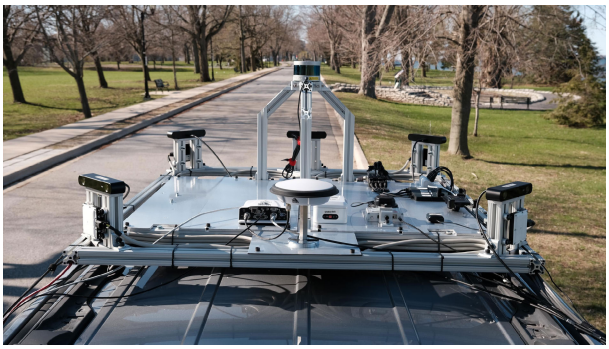

Fig. 2. Frame with sensors mounted on the test vehicle.

TABLE I
EQUIPMENT USED IN THE EXPERIMENTS

	Sensor Type	Update Frequency
IMU	Stereolabs Zed2i IMU	300Hz
Odometer	OBDII	3.5Hz
Radar	UMRR-96	20Hz
Reference Outdoor	KVH IMU with RTK GNSS	50Hz
Reference Indoor	KVH IMU with LiDAR	50Hz

Four electronic scanning radars (ESRs) are located at the four corners of the test bed, angled outward. The test bed is equipped with five Stereolab Zed2i cameras. Each camera contains a low-cost inertial measurement unit (IMU). Images from the front, forward facing camera are used to inspect the surroundings for each scenario. The inertial data from the front forward facing camera also provides the inertial measurement data for the experiments presented in this article. An odometer measuring speed at 3.5 Hz is connected to the vehicle. The sensors used in the presented tests are summarized in Table I.

The ESRs are Smartmicro UMRR-96 automotive radars and provide data at 20 Hz. Scans from all four ESRs are combined and aggregated to form the point cloud used for the ICP-based map registration algorithm. Doppler velocity and target azimuth data from the front-right radar are used within the radar odometry algorithm. The radar odometry algorithm computes the forward velocity of the vehicle as an alternative to the measurements provided by the odometer. The front-right radar is used for radar odometry because all the road tests were undertaken in environments where the right-hand lane is the driving lane. As such, the front-right radar is furthest from the lane containing oncoming traffic and closer to static buildings beside the road.

A. Reference Solutions

The reference system used in the outdoor environments is Novatel PwrPak7-E1, combining a tactical grade IMU (KVH) with a high-precision GNSS receiver (OEM7-SPAN). The solution is postprocessed using Novatel's software Inertial Explorer using corrections from RTK base stations with the recorded IMU/GNSS data.

No GNSS signals are available for use in the indoor environment. Thus, the reference solution for the indoor trajectory is generated using the tactical grade IMU in cooperation with LiDAR-to-map registration. This navigation solution is presented in [20], with the difference being the use of the KVH IMU instead of a low-cost IMU, for heightened precision.

TABLE II
DRIVING SCENARIO STATISTICS

Driving Scenario	1	2	3	4	5
Distance Travelled (m)	1513	743	1187	573	849
Duration (min)	4.6	1.3	14	3.9	1.6
Average Speed (m/s)	5.5	9.3	1.2	2.5	9.2

IV. DRIVING SCENARIOS

Three unique driving scenarios are examined: a shopping street, a university campus, and an indoor parking garage. Statistics for the three trajectories are given in Table II.

Fig. 3 shows side-by-side images and radar scans from each of the three driving scenarios. These figures can be used to compare the manner in which the same scene is perceived by the camera and the radars. It should be noted that these scenarios do not cover elevated driving speeds such as those found on highways. The scenarios are described qualitatively in the following.

A. Scenario 1: University Campus

The first half university campus scenario consists of dormitory buildings and lecture halls, providing ample targets for radar reflections. The second half of the trajectory passes a sports field and the avenue widens significantly, resulting in few radar targets. In the same target-poor section, a large city bus passes the test vehicle, and during this instant, the majority of radar reflections correspond to the bus.

B. Scenario 2: Shopping Street

The shopping street trajectory forms a loop through two main streets in downtown Kingston, ON, Canada. Both streets are one-way, and the test vehicle moves between both driving lanes. Both sides of the streets are lined with parked cars, resulting in map occlusions.

C. Scenario 3: Indoor Parking Garage

The indoor parking garage is challenging due to its high level of symmetry resulting from the repetitive pattern of supporting posts throughout the environment. Roughly half of the parking spaces are occupied by parked cars, and additional cars are moving freely through the garage.

D. Scenarios 4 and 5: Downtown Calgary

The final two trajectories are the most challenging and dynamic of the environments. They lie in downtown Calgary, AB, Canada., and traverse multilane one-way streets. All radars perceive many moving vehicles, and parked cars as well as wide streets make registration with maps a challenge.

V. ANALYSIS

This section examines the performance of radar odometry and map registration across the three driving scenarios. Snapshots of camera images and radar scans for each scenario are shown in Fig. 3.

Fig. 3. Radar and camera snapshots of driving environments. (a) Scenario 1: camera image. (b) Scenario 1: radar scan. (c) Scenario 2: camera image. (d) Scenario 2: radar scan. (e) Scenario 3: camera image. (f) Scenario 3: radar scan. (g) Scenarios 4 and 5: camera image. (h) Scenarios 4 and 5: radar scan.

A. Scenario 1: University Campus

1) Map Registration: The lack of environmental features is a challenge for any perception sensor. Radars are distinct from cameras in that they must have physical objects nearby acting as reflectors for the outputted radio waves. In wide, open spaces, when no such objects are available, the radar will be effectively blind.

Refer to the university campus scenario. Fig. 4 shows a map of Queen's University Campus. The blank area in the mid-right-hand side of the map corresponds to a sports field, and the street widens. In this area, no radar detections are available and the integrated radar-to-map registration algorithm relies fully on INS. The INS solution is seen to drift during this time, as no registration corrections are available. The positioning errors are presented in Fig. 5. Before the sports field, positioning errors are consistently below 2 m but grow drastically once map registration is no longer occurred.

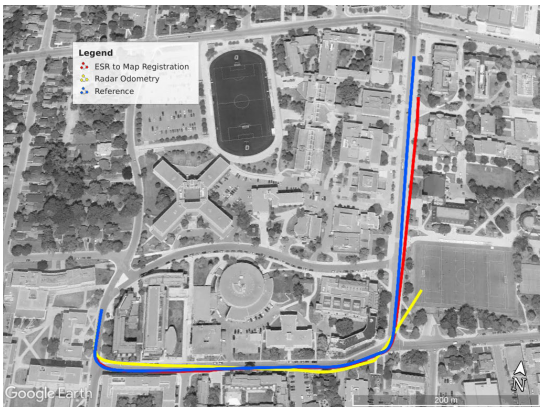

Fig. 4. Scenario 1: map registration and radar odometry compared to the reference.

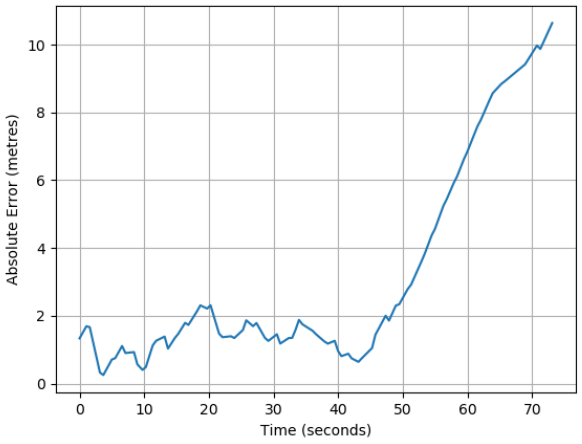

Fig. 5. Scenario 1: absolute errors of map registration solution versus ground truth.

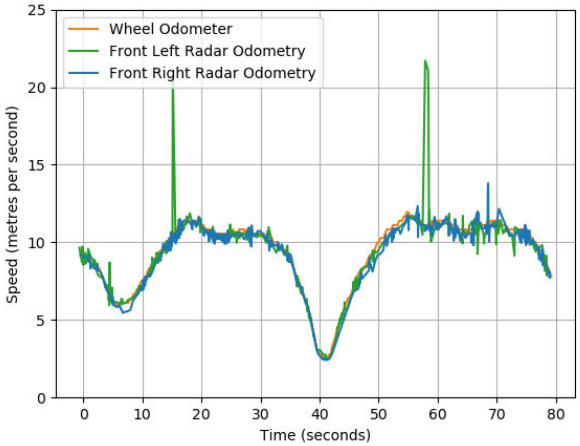

Fig. 6. Scenario 1: radar odometry using front left and right radar, showing spikes in estimated velocity due to dynamic objects.

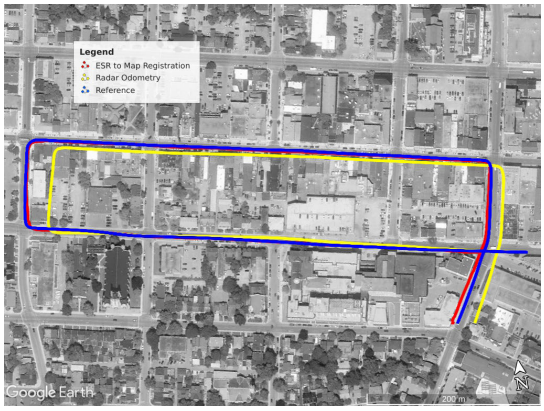

Fig. 7. Scenario 2: map registration and radar odometry compared to the reference.

2) Radar Odometry: Dynamic objects in the neighborhood of an AV have the potential to cause Doppler-velocity-based estimation methods to fail. The Doppler velocity of static objects will have the same velocity profile based on their detected azimuths, satisfying (1). If the largest group of objects with the same velocity profile is static, (2) can be solved successfully for the velocity of the radar. If the largest group of objects is not static, (2) may result in the relative velocity of the moving object.

The effects of a large dynamic object are observed within the driving scenario of a university campus street. Fig. 3(a) shows a city bus in the field of view of the front central camera. Fig. 3(b) shows the same bus as it is perceived by the four radars on the vehicle in one scan. The colored points correspond to the detections of each radar individually. Notice that the bus can be seen clearly as a well-defined rectangle on the left-hand side of the scan. The majority of the yellow points, corresponding to the front left radar, are detections corresponding to the bus. The right-hand radar is a sparse point cloud but does not perceive the bus. Fig. 6 shows the radar odometry estimates from the front left radar.

Compare now the computed velocity estimates in Fig. 6. The bus passes the vehicle at approximately 60 s on the time axis. The velocity computed from the front left radar shown in Fig. 6 shows the velocity spiking to approximately 22 m/s, up from approximately 11 m/s. If the bus and the vehicle are both moving at 11 m/s in opposite directions, their relative velocity would be 22 m/s. The ego-motion estimation is deceived into outputting this relative velocity as the velocity of the vehicle. The same effect is not observed in the solution of the front-right radar because the front-right radar does not detect the bus. Instead, it returns very few detections, and this could contribute to the noise of the outputted velocity estimate around the 70-s mark as well. The earlier spiking in the front left radar is due to a large oncoming vehicle.

B. Scenario 2: Shopping Street

1) Map Registration: In some driving scenarios, objects may obscure the view of map features from perception sensors on the vehicle. Occlusions can include parked cars, moving vehicles, or any object not included in the map.

Fig. 3(c) and (d) shows a camera image and a radar scan from an instant during the shopping street trajectory. Cars line the street, and while radar targets are not sparse, many correspond to parked vehicles and not map features. Fig. 7 shows the radar-to-map registration solution compared to the ground truth trajectory.

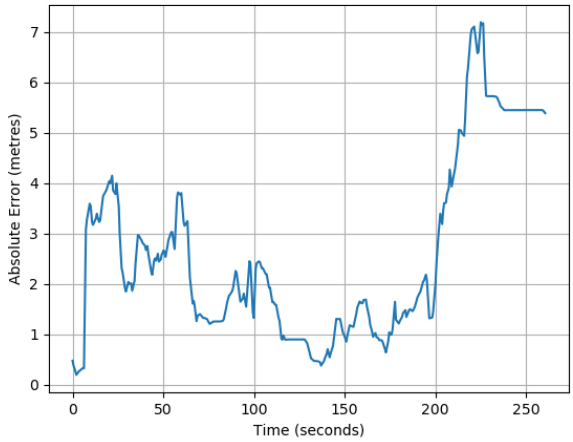

Fig. 8. Scenario 2: absolute errors of map registration solution versus ground truth.

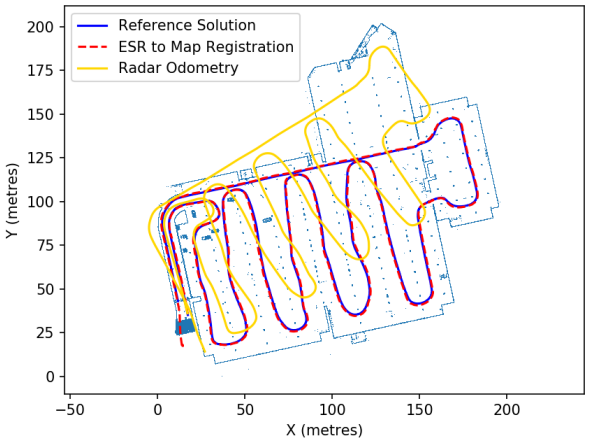

Fig. 10. Scenario 3: map registration and radar odometry compared to the reference.

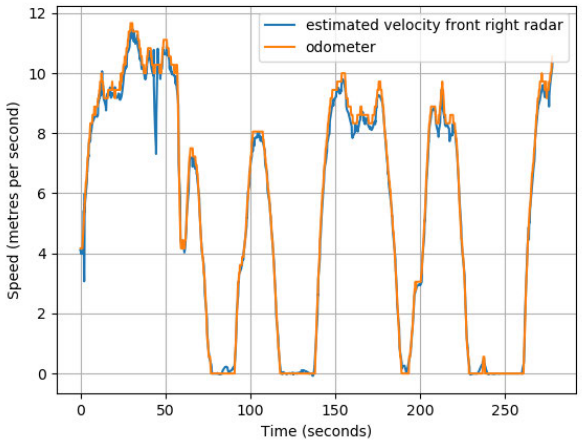

Fig. 9. Scenario 2: radar odometry compared to wheel odometer in an urban environment.

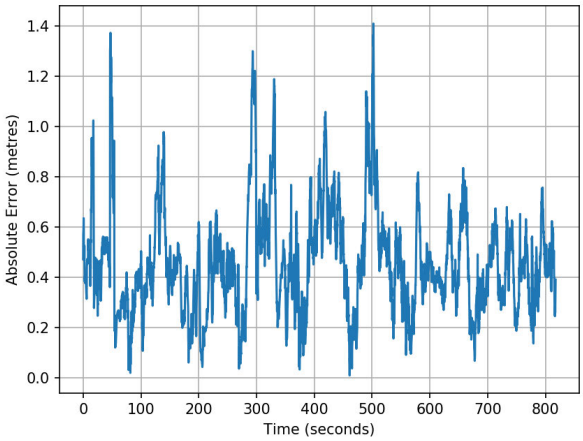

Fig. 11. Scenario 3: absolute errors of map registration solution versus ground truth.

Visually, the trajectory mimics the ground truth closely until the final intersection, but the errors presented in Fig. 8 show that positioning accuracy is inconsistent and relatively high, with a 2-D RMSE of 3.17 m and a maximum 2-D error of 7.58 m. The parked cars lead to false radar-to-map matches and incorrect registration corrections. However, there are features to detect and there is no unbounded position drift.

2) Radar Odometry: Radar odometry estimates for the shopping street are shown in Fig. 9. The radar velocity estimates closely track the measurements from the odometer, with an rms error of 0.31 m/s. The existence of static occlusions does not negatively affect the radar odometry because the algorithm requires only that there should be sufficient static objects. Whether these static objects are reflections from parked cars, trees, or buildings does not impact the radar odometry. In this situation, only radar-to-map registration suffers.

C. Scenario 3: Covered Parking Garage

1) Map Registration: Fig. 10 shows the radar-to-map registration trajectory, comparing the registration solution with the reference solution. The registration algorithm performs robustly in this scenario, maintaining positioning errors of less than 1.5 m 100% of the time and having a 2-D RMSE of 0.5 m. While the high level of symmetry within the garage poses a challenge to the ICP and there are map occlusions in the form of parked cars, the environment is enclosed such that the radars always have sufficient walls and corners supporting meaningful feature detection. Fig. 3(e) and (f) shows a camera image and a radar scan from inside the parking garage, respectively. The 2-D absolute errors are shown for the indoor trajectory in Fig. 11.

2) Radar Odometry: Radar odometry estimates for the indoor driving scenario are shown in Fig. 12. The indoor environment is favorable for radar odometry, providing walls, posts, and static vehicles for reliable velocity estimates. The maximum velocity error is 1.69 m, with an RMSE of 0.33. Vehicles are moving throughout the garage, but when a moving vehicle is detected by the radars, a sufficient ratio of radar detections still corresponds to static objects.

The forward velocity estimate provided by radar odometry is comparatively reliable, but stand-alone radar odometry is not practical for long stretches of time as it is a dead-reckoning solution. Drift in position error accumulates and the result of this is seen in Fig. 10.

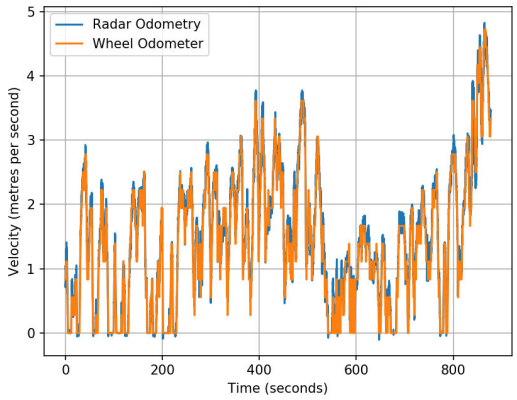

Fig. 12. Scenario 3: radar odometry compared to wheel odometer in an indoor environment.

Fig. 13. Scenario 4: map registration and radar odometry compared to the reference.

D. Scenarios 4 and 5: Downtown Calgary

1) Map Registration: Two driving segments are tested in areas from downtown Calgary, AB, Canada. These environments proved challenging for radar-to-map registration, due to occlusions and wide, multilane streets. Fig. 13 shows the map registration and radar odometry solutions compared with the ground truth. Map registration failed in Scenario 4, and the ICP algorithm was unable to reconverge, resulting in a maximum 2-D error of 21.1 m.

Scenario 5 is presented in Fig. 14. This scenario also resulted in map registration failure, with a maximum error of 17 m.

2) Radar Odometry: The performance of radar odometry in the Calgary scenarios showed comparable performance to the other three trajectories. The forward velocity estimate for Scenario 4 was impacted by moving vehicles in the multilane one-way streets, with a maximum error of 7.97 m/s. However, there were sufficient static reflectors furnished by parked vehicles and buildings to maintain an RMSE of 0.44 m/s. Scenario 5 similarly resulted in an RMSE of 0.40 m/s, with a lower maximum error of 2.43 m/s.

E. Radar at Low or Zero Velocities

A critical feature of automotive radar is its poor performance at zero and near-zero velocities. At these low speeds, radar detections become fewer and noisier [1]. This can be seen

Fig. 14. Scenario 5: map registration and radar odometry compared to the reference.

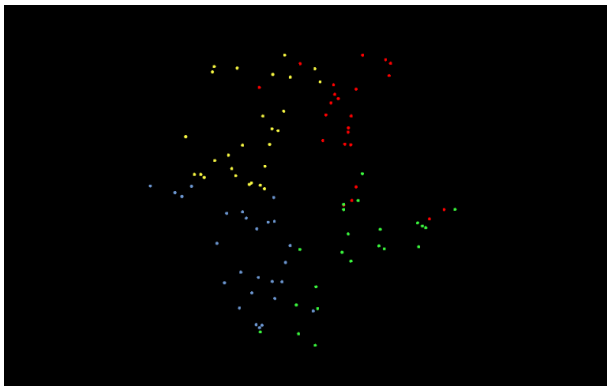

Fig. 15. Radar scan from stationary vehicle.

qualitatively in Fig. 15. Fig. 15 shows a single scan from the indoor parking garage taken when the vehicle is stationary. The radar detections are sparse and distributed across the scene in a near-random way. Compare this to the exact same environment shown in Fig. 3(f). In Fig. 3(f), walls and defined features can be seen clearly. The moment the vehicle stops, the radar scan deteriorates and resembles the scan shown in Fig. 15. Both radar odometry and radar-to-map registration are thus unreliable at zero and near-zero velocities.

Radar scans become sparse at low velocities, as shown in Fig. 15. This can be explored statistically by comparing the number of radar detections per scan to the speed of the vehicle. The challenge is isolating velocity as a variable. Radars excel at detecting moving objects, so the test scenarios need to have limited dynamic objects and rich features to prevent factors such as other vehicles or lack of environmental features from inhibiting the analysis. Therefore, we chose trajectories in our indoor environment to examine how scan length varies with vehicle speed. The range of velocities is divided into ten bins, and for each bin, the average number of detections is computed. The total number of detections considers the point cloud generated at a single update from all four radars. Fig. 16 shows a decline in scan length at speeds below 1 m/s, with fairly consistent scan lengths at speeds higher than this.

F. Numerical Results

The numerical results of radar-to-map registration and radar odometry are summarized in Tables III and IV.

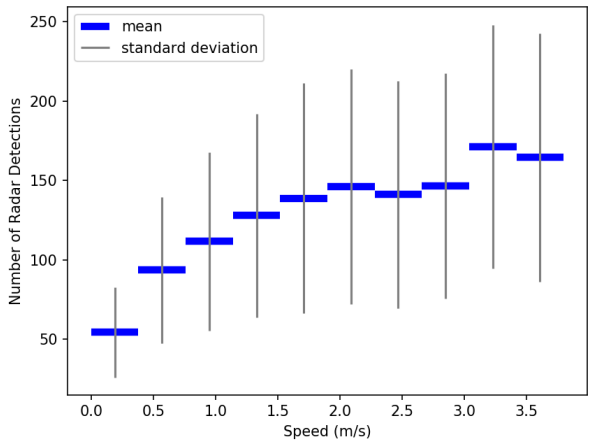

Fig. 16. Mean number of radar detections against binned speed.

TABLE III
NUMERICAL POSITIONING PERFORMANCE OF RADAR MAP MATCHING

Driving Scenario	1	2	3	4	5
2D RMSE (m)	3.17	4.23	0.50	10.79	8.21
2D Max Error (m)	7.58	11.04	1.41	21.10	17.44
% time < 2m error	49%	63%	100%	16.57%	21.29%

TABLE IV
NUMERICAL PERFORMANCE OF RADAR ODOMETRY

Driving Scenario	1	2	3	4	5
2D RMSE (m)	25.7	8.5	29.7	5.57	15.1
2D Max Error (m)	37.6	28.1	65.3	10.85	32.3
Velocity RMSE (m/s)	0.31	0.42	0.33	0.44	0.40
Velocity Max Error (m/s)	2.55	2.91	1.69	7.97	2.43

Overall, the highest positioning accuracy from the map registration algorithm is achieved in Scenario 3, which takes place in a fully indoor environment. While there are moving vehicles present in the environment, they are not as numerous as on the streets of the other scenarios, and the walls are near presenting many radar reflectors. Map registration was able to mitigate position drift in Scenario 2, but failed in Scenario 1 due to lack of features. Map registration also struggled greatly in Scenarios 4 and 5.

The velocity errors are presented for the estimates generated by the front-right radars.

Overall, the scenarios did not present overarching patterns relating to the environment. As long as sufficient static objects are present, whether or not they correspond to map features, radar-based velocity estimation can perform well. Of course, if the majority of radar targets belong to a moving object, radar odometry will fail. This can be mitigated through comparison with additional radar sensors mounted in other locations or with a wheel odometer. As a standalone solution, radar odometry cannot sustain sufficient accuracy for any extended duration of time because it is a dead-reckoning system. It can, however, assist other position fixing methods, such as registration, or bridge short outages.

VI. CONCLUSION

This article presents an implementation and analysis of two radar-based navigation strategies in three diverse driving scenarios. The driving scenarios consist of trajectories through a shopping street, a university campus, and an indoor parking garage. The performance of radar odometry and radar scan-to-map registration is examined across all three scenarios. The challenges faced during the scenarios include dynamic objects, map occlusions, lack of features, and highly symmetric environments. A challenge unique to radar that does not affect cameras or LiDAR is that of noise increase at zero velocity.

Both radar odometry and map registration performed very robustly in the indoor environment, benefiting from abundant objects acting as radar targets. In outdoor environments, radar odometry is reliable when sufficient targets are present such that the algorithm is not deceived by a single large dynamic object. Radar odometry was observed to fail in the university campus scenario when the majority of radar detections corresponded to a city bus. Map registration outdoors was also shown to be more sensitive than indoors, potentially due to the wider nature of outdoor spaces and consequently the sparser radar detections.

As of yet, radar-based navigation methods are not sufficiently precise nor sufficiently robust to serve as a stand-alone positioning method in the absence of GNSS. They do, however, show great potential as a sensor system component to a multisensor positioning system. Automotive radars operate near 77 GHz, corresponding to a wavelength of approximately 4 mm. This characteristic enables the radar signals to easily penetrate through precipitation, ensuring minimal degradation in performance [21]. In contrast, LiDAR predominantly functions within wavelengths ranging from 760 to 1900 nm, making its beams susceptible to reflection and refraction by precipitation droplets [22]. Similarly, the cameras' field of view can be obstructed by precipitation, hampering their ability to detect road features and provide reliable positioning solutions. Due to the robustness of automotive radar to poor lighting and weather conditions, and their ability to provide instantaneous velocity updates, they are a complimentary sensor to cameras and LiDAR.

This work can inform future work in multisensor systems, contributing to decision-making processes that must consider when and how much radar-based navigation should be trusted. Fusing vision point clouds with radar point clouds could marry the higher resolution of the camera with the light and weather resistance of radar.

REFERENCES

[1] L. Narula, P. A. Iannucci, and T. E. Humphreys, "Automotive-radar-based 50-cm urban positioning," 2020, *arXiv:2005.00704*.

[2] T. E. Humphreys, M. J. Murrian, and L. Narula, "Deep-urban unaided precise global navigation satellite system vehicle positioning," *IEEE Intell. Transp. Syst. Mag.*, vol. 12, no. 3, pp. 109–122, Jun. 2020.

[3] A. Noureldin, T. Karamat, and J. Georgy, *Fundamentals of Inertial Navigation, Satellite-Based Positioning and Their Integration*. Cham, Switzerland: Springer, 2013.

[4] U. Iqbal, A. F. Okou, and A. Noureldin, "An integrated reduced inertial sensor system—RISS/GPS for land vehicle," in *Proc. IEEE/ION Position, Location Navigat. Symp.*, Jun. 2008, pp. 1014–1021.

[5] R. Ishikawa, T. Oishi, and K. Ikeuchi, "LiDAR and camera calibration using motions estimated by sensor fusion odometry," in *Proc. IEEE/RSJ Int. Conf. Intell. Robots Syst. (IROS)*, Oct. 2018, pp. 7342–7349.

[6] R. Saussard, S. Zair, and G. Pita-Gil, "Ego-motion estimation with static object detections from low cost radars," in *Proc. 21st Int. Conf. Intell. Transp. Syst. (ITSC)*, Nov. 2018, pp. 1858–1863.

[7] P.-C. Kung, C.-C. Wang, and W.-C. Lin, "A normal distribution transform-based radar odometry designed for scanning and automotive radars," in *Proc. IEEE Int. Conf. Robot. Autom. (ICRA)*, May 2021, pp. 14417–14423.
[8] J. Dickmann et al., "Automotive radar the key technology for autonomous driving: From detection and ranging to environmental understanding," in *Proc. IEEE Radar Conf. (RadarConf)*, May 2016, pp. 1–6.
[9] D. Kellner, M. Barjenbruch, J. Klappstein, J. Dickmann, and K. Dietmayer, "Instantaneous ego-motion estimation using Doppler radar," in *Proc. 16th Int. IEEE Conf. Intell. Transp. Syst. (ITSC)*, Oct. 2013, pp. 869–874.
[10] D. Kellner, M. Barjenbruch, J. Klappstein, J. Dickmann, and K. Dietmayer, "Instantaneous ego-motion estimation using multiple Doppler radars," in *Proc. IEEE Int. Conf. Robot. Autom. (ICRA)*, May 2014, pp. 1592–1597.
[11] A. Pishehvari, U. Iurgel, S. Lessmann, L. Roese-Koerner, and B. Tibken, "Radar scan matching using navigation maps," in *Proc. 3rd IEEE Int. Conf. Robotic Comput. (IRC)*, Feb. 2019, pp. 204–211.
[12] S. H. Cen and P. Newman, "Radar-only ego-motion estimation in difficult settings via graph matching," in *Proc. Int. Conf. Robot. Autom. (ICRA)*, May 2019, pp. 298–304.
[13] E. Ward and J. Folkesson, "Vehicle localization with low cost radar sensors," in *Proc. IEEE Intell. Vehicles Symp. (IV)*, Jun. 2016, pp. 864–870.
[14] S. H. Cen and P. Newman, "Precise ego-motion estimation with millimeter-wave radar under diverse and challenging conditions," in *Proc. IEEE Int. Conf. Robot. Autom. (ICRA)*, May 2018, pp. 6045–6052.
[15] M. Schoen, M. Horn, M. Hahn, and J. Dickmann, "Real-time radar SLAM," in *Proc. Workshop Fahrerassistenzsysteme und automatisiertes Fahren*, 2017, pp. 1–10.
[16] Z. Hong, Y. Petillot, and S. Wang, "RadarSLAM: Radar based large-scale SLAM in all weathers," in *Proc. IEEE/RSJ Int. Conf. Intell. Robots Syst. (IROS)*, Oct. 2020, pp. 5164–5170.
[17] E. Dawson, M. A. Rashed, W. Abdelfatah, and A. Noureldin, "Radar-based multisensor fusion for uninterrupted reliable positioning in GNSS-denied environments," *IEEE Trans. Intell. Transp. Syst.*, vol. 23, no. 12, pp. 23384–23398, Dec. 2022.
[18] M. A. Fischler and R. C. Bolles, "Random sample consensus: A paradigm for model fitting with applications to image analysis and automated cartography," *Commun. ACM*, vol. 24, no. 6, pp. 381–395, 1981.
[19] P. J. Besl and N. D. McKay, "A method for registration of 3-D shapes," *IEEE Trans. Pattern Anal. Mach. Intell.*, vol. 14, no. 2, pp. 239–256, Feb. 1992.
[20] E. Mounier, M. Elhabiby, M. Korenberg, and A. Noureldin. (Jun. 2023). *High-Precision Positioning in GNSS-Challenged Environments: A LiDAR-Based Multi-Sensor Fusion Approach with 3D Digital Maps Registration*. [Online]. Available: https://www.techrxiv.org/articles/preprint/High-Precision_Positioning_in_GNSS-Challenged_Environments_A_LiDAR-Based_Multi-Sensor_Fusion_Approach_with_3D_Digital_Maps_Registration/23280788
[21] F. Kraus, N. Scheiner, W. Ritter, and K. Dietmayer, "Using machine learning to detect ghost images in automotive radar," in *Proc. IEEE 23rd Int. Conf. Intell. Transp. Syst. (ITSC)*, Sep. 2020, pp. 1–7.
[22] J. Kim, B.-J. Park, and J. Kim, "Empirical analysis of autonomous vehicle's LiDAR detection performance degradation for actual road driving in rain and fog," *Sensors*, vol. 23, no. 6, p. 2972, Mar. 2023. [Online]. Available: https://www.mdpi.com/1424-8220/23/6/2972

Emma Dawson received the B.Sc. degree in applied mathematics and engineering from Queen's University, Kingston, ON, Canada, and the M.A.Sc. degree in electrical engineering from the Royal Military College of Canada (RMCC), Kingston. She is pursuing the Ph.D. degree with Queen's University.

She is currently working as a Research Assistant at the Navigation and Instrumentation Research Group (NAVINST), RMCC. Her research interests include sensor fusion, autonomous and vehicular localization, robotic ego-motion estimation, and automotive radar fusion.

Eslam Mounier received the B.Sc. and M.Sc. degrees in computer and systems engineering (CSE) from Ain Shams University, Cairo, Egypt, in 2014 and 2020, respectively. He is pursuing the Ph.D. degree with the Department of Electrical and Computer Engineering (ECE), Queen's University, Kingston, ON, Canada.

He is also a member of the Navigation and Instrumentation Research Laboratory (NavINST), Royal Military College of Canada (RMCC), Kingston. His primary research interests include multisensor navigation systems for autonomous vehicles, advanced machine perception and computer vision techniques, and machine learning and deep learning applications.

Mohamed Elhabiby is currently an Associate Professor with the Faculty of Engineering, Ain Shams University, Cairo, Egypt. He is also the Executive Vice President and the Co-Founder of Micro Engineering Tech, Inc., Calgary, AB, Canada, a high-tech international company specialized in high-precision engineering and instrumentation, mobile mapping, laser scanning, deformation monitoring, and global positioning system (GPS)/inertial navigation systems (INS) integrations. He is the Leader of an Archeological Mission in the Area of the Great Pyramids, Cairo.

Mr. Elhabiby received the Astech Awards. Avenue Magazine named him as one of the Top 40 under 40. He is the Chair of WG 4.1.4: Imaging Techniques, Sub-Commission 4.1: Alternatives and Backups to GNSS. He chaired the Geocomputations and Cyber Infrastructure Oral Session at the Canadian Geophysical Union annual meeting from 2008 to 2012. He was the Treasurer of the Geodesy Section at the Canadian Geophysical Union from 2008 to 2014.

Aboelmagd Noureldin (Senior Member, IEEE) received the B.Sc. degree in electrical engineering and the M.Sc. degree in engineering physics from Cairo University, Cairo, Egypt, in 1993 and 1997, respectively, and the Ph.D. degree in electrical and computer engineering from the University of Calgary, Calgary, AB, Canada, in 2002.

He is a Professor at the Department of Electrical and Computer Engineering, Royal Military College of Canada (RMCC), Kingston, ON, Canada, with cross appointments at the School of Computing and the Department of Electrical and Computer Engineering, Queen's University, Kingston. He is also the Founder and the Director of the Navigation and Instrumentation Research Laboratory, RMCC. He has published two books, four book chapters, and more than 270 papers in journals, magazines, and conference proceedings. His research interests include global navigation satellite systems, wireless positioning and navigation, indoor positioning, and multisensor fusion targeting applications related to autonomous systems, intelligent transportation, road information services, crowd management, and the vehicular Internet of Things. His research led to 13 patents and several technologies licensed to the industry in position, location, and navigation systems.